Implantable Molecular Tracker: Development and commissioning of the electrical system

Philipp Thoma, H. Tom Soh (supervisor), and Bernhard Hollaus (evaluator)

***Abstract*—Gathering physiological and chemical data inside the human body within minutes is key to improve medical treatments and outcomes. This master's thesis focuses on the hardware development of an implantable medical device that integrates a biosensor to measure uric acid inside the human body. Tight spatial boundary conditions in combination with high power requirements pose the main hardware challenges. An LED, combined with collimation and filter optics, triggers the fluorescent biosensors. Low-power electronic readout circuits inside the device translate the emitted fluorescent light signal into a Bluetooth signal. This is read by an external device. After selecting hardware components and designing the PCBs, the electrical and optical system is optimized, including testing the first prototype design. Extensive testing provides precise information about the possible level of detection of the biomarkers, as well as monitors power consumption and battery life. Finally, the devices' electrical characteristic is known. In future, implantable medical devices, like this one, will enable the monitoring and control of biomarkers like uric acid more accurately.**

***Index Terms*—Micro electronic, Implant, Biosensors, 3D-print, Power optimization.**

I. Introduction

BIOMARKERS in the human body are crucial for tracking disease progression and responding to physiological changes [1]. Abnormal uric acid levels, for instance, can indicate gout, kidney stones, and chronic kidney disease [2]. Currently, testing uric acid levels requires a blood sample, with patients needing to fast for four hours before the test [2]. The results, typically available within 24 hours, involve laboratory analysis [3].

P. Thoma studies in the Department of Mechatronics, MCI, Innsbruck, Austria, e-mail: ph.thoma@mci4me.at.

Continuous monitoring using an implantable or ingestible sensor simplifies this process, providing real-time measurements that reveal concentration gradients and trace medication effects. Interstitial fluid (ISF) surrounds tissue cells and contains a biomarker composition similar to blood, making it an accessible medium for monitoring. ISF-based continuous glucose monitors detect less than a 10% absolute relative difference from blood-based glucose meters [4].

Implantable sensors offer medics a extensive view of patient's conditions. While blood samples provide snapshots, implantable devices track biomarkers continuously, showing variations and responses to specific events, leading to more targeted treatments. Designing a reliable, efficient, and biocompatible implant, however, presents significant challenges.

For this project, fluorescent labeled aptamers are utilized as affinity reagents. Aptamers are single-stranded DNA or RNA oligonucleotides that bind to proteins with high specificity [5]. They are preferable due to their high stability, low cost, and high specificity compared to other affinity reagents like antibodies and others. Aptamers can be designed and reproduced to target almost any protein [5].

The aptamers are bound to a 3D-printed scaffold, with packing density being the main size constraint. Using fluorescent labeled aptamers require both excitation source and emission detection. Collimation and focusing lenses enhance the output signal intensity, while optical filters minimize excitation light leakage into the emission band. The electrical system, which includes a battery, radio, excitation LED, and emission sensor, is essential for the implant's functionality. This integration of optical and electrical

components is crucial for reliably monitoring uric acid levels in interstitial fluid.

This project aims to develop a baseline implantable sensor that can be easily adapted for measuring various biomarkers. Once the initial setup is completed, the required LED power for detecting different biomarker concentrations can be recorded. The hardware will then be compatible with aptamers designed for other biomarkers, making the system versatile. Uric acid measurement and the current diameter are just starting points. As technology advances and aptamer packing density increases on the scaffold, the device size can be reduced, potentially leading to the creation of an ingestible sensor.

This paper reviews current ingestible electric capsules and aptamer switches before detailing our device's specifications, including the electrical system (battery, radio, excitation LED, spectral sensor), optical system (filters, lenses), and enclosure. We outline our approach to integration and realization, followed by the presentation of test results. The paper concludes with a discussion for the sensor technology and presenting the remaining problems alongside the achieved baseline.

II. State of the art

A. Ingestible electric capsules

Ingestible pills and implantable sensors share very similar technological challenges, making it relevant to analyze currently available ingestible products to design of a high quality implant.

Existing ingestible electronic pills on the market are designed for measuring body core temperature, detecting fluorescence, or performing video endoscopy. Most pills are used for video endoscopy. Relevant products in this area include Medtronic PillCam SB3 [6], Intro-Medic MiroCam [7], and others such as those by the Jinshan group [8], Olympus [9], CapsoVision [10] and RF SYSTEM lab [11]. Capsules used for infrared fluorescence cancer screening and fluorescence capsule endoscopy are more closely aligned with the concept of the implantable molecular tracker (IMT), though they still utilize different measurement techniques. Both types detect fluorescence optically, but one relies on an externally introduced fluorophore that reacts with tissue [12], while the other utilizes autofluorescent substances like flavin adenine dinucleotide (FAD) [13]. The latter also employs an application-specific integrated circuit (ASIC) chip, making the design especially compact.

B. Implantable sensors

Several continuous glucose monitoring implants are currently available, all powered wirelessly using a second, rechargeable device placed just above the implanted sensor. One example is the Senseonics Eversense E3, which also uses an ASIC chip to minimize the implant's size [14]. Despite these advancements, there is no device available yet that measures biomarkers, specifically uric acid, in the ISF.

C. Aptamer switches

Aptamers are single-stranded DNA or RNA oligonucleotides. They bind to proteins with high affinity and offer high specificity and stability, which are crucial for developing reliable biosensors [5]. Reversible binding makes aptamers the perfect fit for continuous measurements of changing concentration. The use of fluorescent labeled aptamers enhances detection sensitivity, allowing for precise measurement of biomarker concentrations. This technology is particularly relevant for the development of sensors that can monitor various biomarkers continuously and in real-time.

III. Materials and methods

Figure 1 shows the final arrangement of components inside the IMT. The collimated and filtered LED light excites the fluorophores attached to the aptamers in the measurement chamber. The fluorophores absorb the excitation light and emit light in a shifted, longer wavelength spectrum. Emission optics are required to reduce excitation leakage to

the light sensor, which measures the emission light intensity.

Debugging capabilities and maintainability are important for the electrical system. Firmware must be developed and tested for the radio chip. The working electrical system then needs to be united with the optics and everything housed in a custom enclosure. The integrated system is designed to meet key requirements:

- Battery life: At least $8\,\mathrm{h}$.
- Bluetooth functionality: Custom service to send measurement data to a connected device.
- Biocompatibility: Ensured for safe interaction with human tissue.
- Size: $40\,\mathrm{mm}$ in length, $27.5\,\mathrm{mm}$ in diameter.

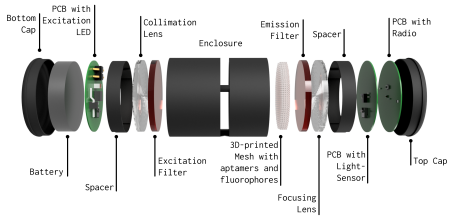

Figure 1: Explosion drawing of the implantable molecular tracker.

A. Electrical system

In the project's initial phase, the foremost priorities encompassed the development of the electrical schematic and layout. A preliminary search for suitable radio chips was conducted, followed immediately by the design of the printed circuit boards (PCBs). Upon arrival of the custom PCBs, basic functionality was tested to ensure their quality. Key components of the electrical system include:

- Radio Module: ISP2053 with matched antenna and integrated peripherals.
- Light Sensor: AS7341, with separated channels for excitation and emission wavelengths.
- Excitation LED: SST-10-R-B130 to excite fluorescent labeled aptamers.
- Battery: LIR2032, $3.7\,\mathrm{V}$, $70\,\mathrm{mAh}$ rechargeable lithium-ion battery.

Only silver oxide batteries have the authorities approval for implants, but they don't meet the power requirements for this prototype. Therefore, a lithium-ion battery, type LIR2032, is selected to provide proof-of-concept state of the overall system.

B. Software development

Software development commenced using the ISP2053-AX-EB and AS7341 evaluation kits, provided by the radio-chip and sensor manufacturers, allowing for functional development while waiting for the custom boards to be manufactured. I2C and Bluetooth communication were integrated, along with sensor setup and data reading. The data from the chip is sent to a connected Bluetooth device. It is possible to connect android phones and iPhones, utilizing the *nRF Connect* app, or a windows computer, using a custom python script. The python script is developed to enable data logging in a .csv file, facilitating easy analysis and review of the collected data.

With the custom PCBs, current consumption was tested and optimized. The process is depicted in figure 2, starting at an average current consumption of $2.35\,\mathrm{mA}$ and improving it to $0.508\,\mathrm{mA}$, by activating the power management configuration and a Low Drop Out (LDO) regulator, instead of the DCDC.

C. Optics development

The optics development focused on selecting the appropriate lenses and filters. The two required filters are specifically matched to work well with the fluorophore Cy5, blocking as much excitation light as possible, while not blocking the emission wavelength for the sensor. To save weight and space, acrylic Fresnel lenses were chosen. With a focal length of $5\,\mathrm{mm}$ and a diameter of $25\,\mathrm{mm}$, these lenses match the required distance between the light source and the sample, ensuring full illumination of the sample,

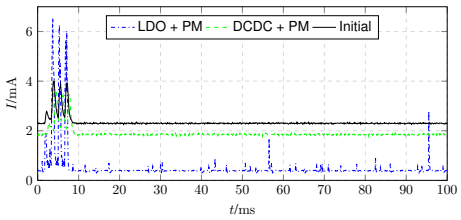

Figure 2: Progress in current consumption of the IMT, by changing the power management (PM) and peripheral power setup.

when using a 130° emitting light source [15]. Optical lenses serve two essential purposes in the implant: Collimation or focus of light, enhancing incident power. And reduction of the angle of incidence on the filters, ensuring their optimal performance.
Figure 3 shows the incident power on a *Thorlabs* PM400 power meter for different distances s and different optical setups. The distance axis shows the distance between the power meter and the LED, or the lens, respectively. Using no collimator lens results in the dashed line. Comparing it to the power, using a collimator lens (dash dotted line), it is obvious that a lens is important for small distances already. Perfect collimation would result in constant power over distance. Though not perfect, the selected Fresnel lens collimates sufficiently. Distance in the implant will be $14\,\mathrm{mm}$, making the lens the best option. Adding the excitation filter to the setup reduces the power marginally, as a small part of the emitted spectrum is blocked by the filter.
The final optical system features:

- Lens: Fresnel lens with
  - effective Focal Length of $5\,\mathrm{mm}$,
  - diameter of $25\,\mathrm{mm}$,
  - center thickness of $2\,\mathrm{mm}$ and
  - groove density of 250 grooves per inch [15].
- Filters:
  - Excitation Filter: SEMROCK 628/40
  - Emission Filter: SEMROCK 692/40
- Spacer:
  - $4.6\,\mathrm{mm}$ height,
  - cutout for the cable and
  - support structure to increase stability.

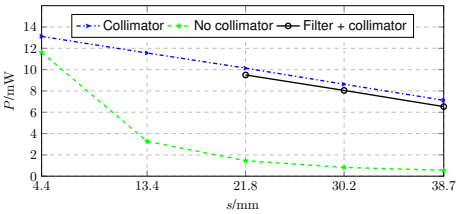

Figure 3: Incident power with and without collimating optics.

D. Enclosure

The enclosure development process involved iterative testing with different 3D printed designs to ensure minimum weight, while also keeping the structural integrity and functionality in mind. Various wall thicknesses, closing mechanisms, and arrangements were tested to achieve an optimal balance of durability and functionality. This iterative process was crucial to develop a reliable and robust enclosure for the electrical and optical system. The *Carbon M2* 3D printer and UMA90 resin were used for all different designs.
Figure 4 shows the final enclosure design. The two compartments left and right of the sample-slit must be connected, as sensor and excitation LED must be on opposite sides of the sample. Therefore, the tunnel, visible in the left picture of figure 4, is integrated, making sure a cable can connect both compartments electrically, without any sealing issues. On the right hand side in figure 4, the connection between the main enclosure and the end cap is visible. The two parts slide into each other and need to be fixed and sealed with glue. *Loctite* 4902 is a biocompatible, fast curing adhesive, that works well for this IMT [16].

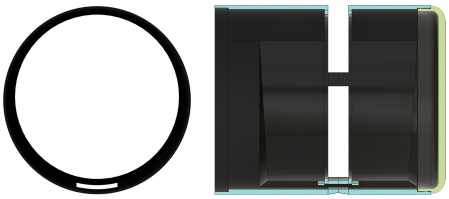

Figure 4: Rendering of enclosure in different views, highlighting the design features.

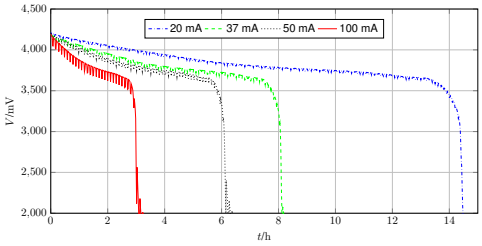

Figure 5: IMT battery life for different LED currents with 5 s intervals and 1 s LED turn on time.

IV. Results

A. Battery life

Figure 5 shows the battery life of the IMT for four LED currents. The LED is turned on with the respective current for 1 s in 5 s intervals. During the remaining 4 s of the interval, a standby current of 508 µA is consumed. As a result, doubling the LED current does not exactly half battery life. The standby current is especially relevant for low LED currents, since the average current drawn is lower overall. For the later use case of the IMT, the time between starting two measurements will be much longer than 5 s, increasing the standby currents importance. However, the battery life will benefit from this change, as the average current drawn will be lower. The initially set target of a 8 h battery life is met with currents lower than 37 mA for 5 s intervals.

No matter the LED current, eventually the battery is fully drained and the cell voltage of the lithium ion battery drops significantly, below 2 V. If that happens, the electrical system switches into a parasitic battery saving state. The LED, in combination with the LED driver, needs about 2 V forward voltage to draw a significant current. If the LED is turned on, the battery voltage drops further, due to the increased load. The combination of these aspects leads to the LED not being turned on after the battery voltage dropped below 2 V. This reduces the current drawn from the battery and prevents very deep discharge.

B. Limit of detection

For the limit of detection (LOD) test, pure Cy5 dye is diluted in water. From the initial concentration of 2 mM, the dilution is done in four steps, finally reaching 1 fM as the lowest concentration. The 30 mL water were poured by hand. The goal is to find the detectable order of magnitude rather than exact values, making this approach sufficient. As a reference level, one measurement using water was performed, before the IMT got dropped into the different Cy5 solutions. Higher concentration solutions were pipetted into the solution to increase the concentration by one and two orders of magnitude, before putting the IMT into the next cup with higher concentration. For every concentration, different LED currents were setup. To make sure no errors were made, all measurements were performed twice with entirely new dilutions and a new IMT.

Looking at the lowest measured concentrations, figure 6 shows the results of the 20 mA LED current measurement from both datasets. All axis use logarithmic scale. Thus, ideally the measurement data should resemble a line with constant slope, which it does not. The dashed lines in blue and green indicate plus minus three standard deviations of the average ADC value for water, the dotted lines indicate plus ten times the standard deviation of the water baseline measurement for each dataset. Each measurement value also indicates plus minus one standard deviation around the average value. The

three standard deviation barrier is defined here as the LOD, ten times standard deviation as the limit of quantification (LOQ). For $1\,\mathrm{pM}$ in dataset 2, the measurement failed, which was only realized after the experiment was finished. Therefore this measurement is deleted out of the graph.
Considering the thresholds for LOD and LOQ, the LOD is $1\,\mathrm{fM}$ and LOQ is $10\,\mathrm{fM}$. The ADC value for water changed from 187 ticks to 323 ticks between the measurements. But if the two are plotted in the same diagram, like in figure 6, both show the same pattern. This shows the importance of a water baseline calibration, to get reliable results.

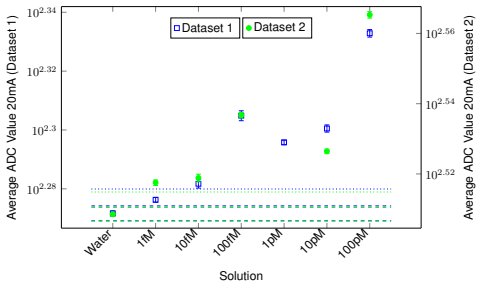

Figure 6: Cy5 diluted in water, concentration with error bars for each measurement and indicated water baseline. Dashed line indicates 3σ, dotted line 10σ.

C. In vitro

Initial tests of the IMT with a scaffold with aptamer switches attached to it, were performed in vitro. For that, a scaffold was fixed to the measurement chamber of an IMT. Two cups, one containing deionized (DI) water, the other a buffer solution were prepared to fully submerge the IMT.
DI water activates all the aptamer switches, while the buffer solution deactivates them. Figure 7 shows the measurement data. At $t = 0$ the IMT was submerged in the DI water. At $t = 300\,\mathrm{s}$, transition to the buffer solution was done. At $t = 600\,\mathrm{s}$ it was put back into the DI water. The measurement was done continuously with a $0.2\,\mathrm{Hz}$ frequency and $50\,\mathrm{mA}$ LED current.
The dip at $t = 600\,\mathrm{s}$ is most likely due to the IMT not being fully submerged in either of the liquids during the switch. Nonetheless, it is clearly visible how the signal changes over time, with the liquids diffusing into the scaffold and reacting with the aptamer switches. For the buffer, it seems like the $5\,\mathrm{min}$ interval is enough to switch off almost all aptamers, barely changing the signal at the end. For the DI water it looks like the IMT should have stayed in the DI water for longer, as the signal ramps up with almost constant gradient all the time. The second time, the IMT is in the DI water, the gradient of the signal is lower than the first time. This might be the result of buffer still being in the scaffold and the water having to first counteract the buffers effects. The difference between highest and lowest measurement value is in the range of 1000 ADC ticks, which is about $1.5\,\%$ of the dynamic range available. Considering that this is the maximum possible signal amplitude, this is not too promising.

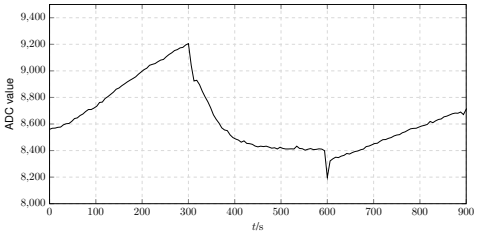

Figure 7: In vitro measurement signal over time with aptamer switches, changing from deionized water to 1x buffer and back to deionized water in $5\,\mathrm{min}$ intervals.

D. In vivo

Nonetheless, in vivo experiments with rats were conducted to see the aptamers work in real conditions, and test the surgery's complexity. Figure 9 shows the IMT being implanted in the interstitial area on the back of an anesthetized rat.

Figure 8: IMT implanted into a rat.

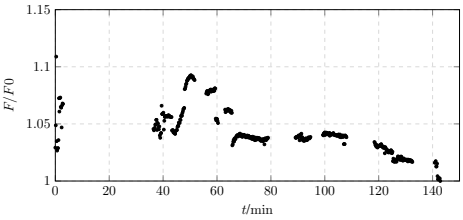

Figure 9: In vivo measurement signal over time with aptamer switches, rat awake. The measurement stopped several times for unknown reasons, when run on a Mac resulting in the gaps in the plot. Values are normalized to the lowest measurements value.

Figure 9 shows the results from the first IMT implantation in a rat. The data is normalized to the lowest measurement value. During the recording there were issues with the macOS environment, randomly stopping the measurement, resulting in the big gaps between some data points.
At approximately $t = 40\,\mathrm{min}$, the rat began moving around in its enclosure. Although the uric acid level remained constant, big changes were detected in the measurements, likely due to increased contact between the IMT and ISF from moving. From $t = 70\,\mathrm{min}$, the rat became inactive again, resulting in stable measurement values. The signal decrease at the end could be due to photobleaching of the fluorophores, but this was not specifically investigated at this stage.

V. Conclusion

The primary goal of this thesis was to develop a functional prototype of an optical implant for measuring uric acid levels in ISF. This required the development of electronics and firmware to achieve at least $8\,\mathrm{h}$ of battery life, along with the selection of suitable optical components and the design of an enclosure to protect the system within the ISF environment. The successful creation of this prototype demonstrates the feasibility of using aptamers with reversible binding to monitor changing biomarker levels, with uric acid serving as the initial focus. This technology holds promise for future projects targeting other, more critical, biomarkers, such as cardiac troponin.

The electrical system operates with a standby current of $508\,\mu\mathrm{A}$. Bluetooth functionality allows for remote adjustment of LED current, measurement intervals and sensor integration times. Tests revealed a battery life of up to $14\,\mathrm{h}$ for $20\,\mathrm{mA}$ LED current, at measurement intervals of $0.2\,\mathrm{Hz}$ and $20\,\%$ LED on time. Achieving a limit of detection of $1\,\mathrm{fM}$ and limit of quantification of $10\,\mathrm{fM}$ for Cy5 molecules in water highlights the potential of this system.

Challenges remain, particularly in reducing standby current to extend battery life and scaling down the hardware for human application. Future work will focus on minimizing the implant size while maintaining or improving performance, potentially through wireless power transfer. The implantable molecular tracker developed in this project offers a versatile platform for testing various aptamers, laying the groundwork for real-time biomarker monitoring that could revolutionize healthcare, much like glucose monitors have today.

Acknowledgment

I would like to express my gratitude to my supervisor, FH-Prof. Bernhard Hollaus, PhD, for his

invaluable guidance, support, and encouragement throughout this project.
I am also deeply thankful to Prof. Dr. H. Tom Soh for welcoming me into his research group and for his mentorship, which has significantly enriched my experience. I extend my thanks to the entire Soh lab for their collaboration, support, and for fostering a welcoming environment.
I am also grateful to the Austrian Marshall Plan Foundation for their financial support, which made this project possible.

REFERENCES

[1] O. Adeniyi *et al.* (2021) Monitoring biomarker. [Online]. Available: https://www.ncbi.nlm.nih.gov/books/NBK402282/
[2] N. J. Gonter. (2023) Uric acid - blood. [Online]. Available: https://medlineplus.gov/ency/article/003476.htm
[3] S. Thompson. (2021) How long does it take to get results of blood tests? [Online]. Available: https://nortonhealthcare.com/news/how-long-do-blood-test-results-take/
[4] M. Friedel *et al.*, "Opportunities and challenges in the diagnostic utility of dermal interstitial fluid," *Nat. Biomed. Eng*, no. 7, p. 1541–1555, 2023.
[5] L. Cohen and D. R. Walt, "Highly sensitive and multiplexed protein measurements," *Chemical Reviews*, vol. 119, no. 1, pp. 293–321, 2019, pMID: 30152694. [Online]. Available: https://doi.org/10.1021/acs.chemrev.8b00257
[6] Medtronic. (2019) Pillcam™ sb 3 capsule endoscopy system. [Online]. Available: https://www.medtronic.com/covidien/en-us/products/capsule-endoscopy/pillcam-sb3-system.html
[7] IntroMedic. (n.d.) Innovative capsule endoscope. [Online]. Available: https://www.medtronic.com/covidien/en-us/products/capsule-endoscopy/pillcam-sb3-system.html
[8] L. Chongqing Jinshan Science & Technology (Group) Co., "Capsule endoscopy system," https://www.jinshangroup.com/uploads/file/2024-01-24/HD_Brochure_1023.pdf, 2023.
[9] Olymups, "Smart and safe, endocapsule 10," https://mdc.olympus.eu/asset/084438885177/5d0af142e2e8473ef0654924591fe3ae, 2021.
[10] C. Inc. (2023) Capsovision product specifications. [Online]. Available: https://capsovision.com/physicians/product-specifications/
[11] L. RF Co. (2018) Sayaka the next generation capsule endoscope. [Online]. Available: https://rfsystemlab.com/en/sayaka/
[12] P. Demosthenous, C. Pitris, and J. Georgiou, "Infrared fluorescence-based cancer screening capsule for the small intestine," *IEEE Trans Biomed Circuits Syst.*, vol. 10, no. 2, pp. 467–476, 2016. [Online]. Available: https://ieeexplore.ieee.org/stamp/stamp.jsp?tp=&arnumber=7217853&tag=1
[13] M. A. Al-Rawhani, J. Beeley, and D. R. S. Cumming, "Wireless fluorescence capsule for endoscopy using single photonbased detection," *Sci Rep*, vol. 5, no. 18591, 2015. [Online]. Available: https://www.nature.com/articles/srep18591citeas
[14] S. J. Walters, "Senseonics the next generation of continuous glucose monitoring," https://www.senseonics.com/ /media/Files/S/Senseonics-IR/documents/publications/uk-public-health-service-publication.pdf, n.d.
[15] EdmundOptics. (n.d.) 0.98 x 0.98 0.20 focal length, fresnel lens. [Online]. Available: https://www.edmundoptics.com/p/098-x-098-020-focal-length-fresnel-lens/42289/
[16] Henkel. (n.d.) Loctite® 4902. [Online]. Available: https://next.henkel-adhesives.com/us/en/products/industrial-adhesives/central-pdp.html/loctite-4902/Loctite4902.html

Philipp Thoma is a Master's student of the Mechatronics program at MCI Innsbruck, Austria. He conducted his research for this paper as a Visiting Student Researcher in the electrical engineering department at Stanford University.